Journal of Crystal Growth 340 (2012) 34–40

Contents lists available at SciVerse ScienceDirect

Journal of Crystal Growth

journal homepage: www.elsevier.com/locate/jcrysgro

Microstructure of PAMBE-grown InN layers on Si(1 1 1)

R. Walther [a,*], D. Litvinov [a,b], M. Fotouhi [a], R. Schneider [a], D. Gerthsen [a,b], R. Vöhringer [b,c], D.Z. Hu [b,c], D.M. Schaadt [b,c,1]

[a] Laboratorium für Elektronenmikroskopie, Karlsruher Institut für Technologie (KIT), D-76128 Karlsruhe, Germany
[b] Center for Functional Nanostructures, KIT, D-76128 Karlsruhe, Germany
[c] Institut für Angewandte Physik, KIT, D-76128 Karlsruhe, Germany

ARTICLE INFO

Article history:
Received 13 July 2011
Received in revised form
9 November 2011
Accepted 26 November 2011
Communicated by M. Tischler
Available online 4 December 2011

Keywords:
A1. Crystal structure
A1. Defects
A1. Meltback etching
A3. Molecular beam epitaxy
B1. Nitrides
B2. Semiconducting III/V materials

ABSTRACT

The microstructure of InN layers grown by plasma-assisted molecular beam epitaxy on Si(111) substrates and an AlN buffer layer was investigated. InN layers with a thickness of ~500 nm were deposited at substrate temperatures between 325 °C and 375 °C under otherwise identical conditions. The structural characterization was performed by scanning electron microscopy and different transmission electron microscopy techniques including selective-area electron diffraction, electron-energy loss spectroscopy and energy-dispersive X-ray spectroscopy. The microstructure of the InN layers changes considerably despite the comparably small interval of growth temperatures.

1. Introduction

InN is a promising material due to its extraordinary physical properties such as small direct band gap of 0.7 eV, low effective electron mass, high electron mobility and high saturation velocity [1–3]. Therefore it is well suited for applications in high-speed optoelectronic devices—provided that material with good structural quality can be produced. Furthermore the ternary InAlN and InGaN alloy systems allow band-gap tuning over a wide spectral range from ultraviolet (AlN) to infrared (InN), including the whole visible spectrum, enabling applications like high-efficiency multi-junction photovoltaic devices. Alloyed with Mn, InMnN becomes a dilute magnetic semiconductor, extending the range of application to spintronics [4]. Recent reports show THz generation [5,6] as well as viable thermoelectric properties [7–11] of InN and its alloys, further enlarging the range of applications of group-III nitrides.

The most common substrate for InN growth is Al_2O_3(0001), which is disadvantageous due to the high lattice-parameter mismatch of 28% and different thermal expansion coefficient. Moreover, its high resistivity prevents the direct electrical connection of InN devices with electronic components in the substrate. Recent research interest focuses therefore on the growth of InN on other, more suitable substrates, including silicon. Its advantages are a reduced lattice-parameter mismatch of only −7.7% for InN growth and excellent crystal quality. Another strong motivation for InN on Si(111) growth is the possible combination of InN-based devices and electronic devices, which can be implemented in the substrate by the well-established Si-technology.

Despite these advantages only few studies regarding the growth of InN on Si(1 1 1) substrates were published up to now. Hsiao et al. [12] reported that nitrogen-rich plasma-assisted molecular beam epitaxy (PAMBE) growth conditions lead to grainy, polycrystalline InN films whereas a N/In-ratio near stoichiometric conditions results in two-dimensional (2D) layer growth. A low-temperature InN buffer layer yields a poor crystal quality whereas a high-temperature AlN (HT-AlN) buffer layer improves the structural quality of the InN epilayer. Grandal and Sánchez-García [13] studied the influence of the growth temperature on the InN growth by PAMBE. Growth above 500 °C near the dissociation temperature leads to In-droplet formation on the surface. Below 500 °C, the growth process could be controlled by the N/In-ratio. They also reported uncoalesced, polycrystalline morphologies for N-rich growth conditions whereas increasing the In/N-ratio leads to coalesced columnar growth. Inverse pyramidal structures resulted from the growth without a buffer layer, indicating an inefficient wetting process. The deposition of a low-temperature InN (LT-InN) layer or a HT-AlN-buffer layer produced coalesced epilayers with superior crystal quality. Ajagunna et al. [14] managed to grow compact InN layers directly on Si(111) by RF-MBE under nearly stoichiometric conditions. However, the

* Corresponding author. Tel.: +49 721 608 48682; fax: +49 721 608 43721.
E-mail address: roman.walther@kit.edu (R. Walther).
[1] Present address: Institut für Energieforschung und Physikalische Technologien, Technische Universität Clausthal, Am Stollen 19B, 38640 Goslar, Germany.

0022-0248/$ - see front matter © 2011 Elsevier B.V. All rights reserved.
doi:10.1016/j.jcrysgro.2011.11.068

sample exhibited weak adhesion to the substrate. A LT-InN buffer layer improved adhesion but small voids were introduced at the InN/Si-interface. The highest quality InN epilayers were obtained by the deposition of a GaN/AlN-bilayer buffer. Sakalauskas et al. [15] also studied PAMBE growth of InN on Si(111) and sapphire substrates. For the samples grown on Si(111) with a HT-AlN-buffer layer they reported a narrower FWHM (917 arcsec) of the InN(0002) reflection measured by X-ray diffraction (XRD) compared to a GaN/AlN-buffer layer (973 arcsec). InN grown on a commercial lumilog GaN:Si on sapphire template with an additional GaN buffer layer yielded an InN(0002) FWHM of 512 arcsec.

Recent advances in metal organic vapor phase epitaxy (MOVPE) growth have also lead to high-quality InN layers. Jamil et al. [16–18] reported MOVPE growth of InN on GaN/Al_2O_3(0001) and GaN/Si(111) templates. The FWHM of the InN(0002) reflection for the GaN/Al_2O_3(0001) template was reported as 281 arcsec, indicating high crystal quality [16]. The crystal quality of InN on the GaN/Si(111) template was worse compared to the GaN/sapphire template as indicated by a higher surface roughness and the presence of metallic In reflections in XRD scans.

Despite the large lattice-parameter mismatch between AlN(0001) and Si(111) of -19% and between InN and AlN of $+13.9\%$, the introduction of an AlN-buffer layer improves the crystal quality of the InN layer. The strain at the AlN/Si(111) interface is relieved by an approximate lattice matching of 5 AlN-crystal planes to 4 Si-crystal planes leading to the introduction of geometrical misfit dislocation arrays. The same mechanism accounts for (partial) strain relief at the InN/AlN interface where approximate lattice matching is achieved for a 7:8-ratio of AlN- to InN-crystal planes [19].

In this work we have studied the microstructure of InN epilayers grown on Si(111) substrates by PAMBE. The InN layers were deposited on AlN-buffer layers with optimized structural properties [20]. The substrate temperature for the InN deposition was systematically varied between 325 °C and 375 °C under otherwise unchanged conditions. The microstructure was analyzed by scanning electron microscopy (SEM), X-ray diffraction (XRD) and transmission electron microscopy (TEM) combined with energy-dispersive X-ray spectroscopy (EDXS) and electron-energy loss spectroscopy (EELS). The InN layers exhibit a complex microstructure, which changes significantly even within the comparably small interval of substrate temperatures. We have in particular observed and analyzed for the first time inclusions in the substrate and InN layer, which are proposed to be formed by a complex meltback reaction.

2. Experimental details

InN epilayers were grown on Si(111) substrates using a RIBER Compact 21T equipped with an Oxford RF Atom Source H25 nitrogen-plasma source and a standard Knudsen effusion cell for indium. Prior to growth the substrate was rinsed twice in acetone and isopropanol to remove organic contaminants. Subsequently the substrate was chemically cleaned in a HF:H_2O (1:50) solution to remove surface oxide layers. After transfer to the loading chamber the substrate was degassed at 130 °C for 60 min before the transfer to the growth chamber. The temperature was ramped up to 900 °C, allowing the substrate to deoxidize for 30 min. Furthermore the transition from the 7×7 Si-surface reconstruction to the 1×1 reconstruction was observed by reflection high-energy electron diffraction (RHEED). Prior to the growth of InN, an AlN-buffer layer with a thickness of $\sim$30 nm was deposited at 880 °C. The Al-cell temperature was set to 1122 °C and the excitation energy of the N-source was set to 400 W with a flux of 0.4 sccm. Under these conditions, AlN-buffer layers with a smooth surface are obtained. Three different samples, P325, P350 and P375, were grown at substrate temperatures of 325, 350 and 375 °C, respectively, keeping all other parameters fixed. The In-cell temperature was 810 °C, the N-source was excited with 400 W with a flux of 0.5 sccm. The N/III-ratio was controlled via the temperature of the Knudsen effusion cell, the plasma-source excitation energy and the nitrogen flux. All samples were grown in the metal-rich growth regime. The III/N-ratios were determined from post-growth measured beam-equivalent pressures of the constituents. Although the cell parameters were kept constant for all samples, post-growth measurements of the Al/N-ratio indicated that the Al/N-ratio could have been higher due to fluctuations of the cell temperature.

XRD-rocking curves of the (0002) reflection were acquired with a Bruker-AXS D8 Discover diffractometer. SEM was employed to study the surface morphology of the samples. Cross-section TEM specimens were prepared by mechanical grinding and Ar^+-ion polishing. The TEM cross-section samples contain two specimen pieces along the [1 − 10]- and [112]-zone axes of silicon which are oriented perpendicular with respect to each other. Bright-field (BF) and dark-field (DF) TEM imaging as well as high-resolution TEM (HRTEM) etc. was performed using a Philips CM 200 FEG/ST operated at 200 kV. Energy-filtered TEM (EFTEM) images were recorded using a Zeiss 922 Omega [21]. EDXS was performed in an FEI Titan^3 80-300 to determine the chemical composition with high spatial resolution. Composition-sensitive images were taken by high-angle annular dark-field scanning transmission electron microscopy (HAADF STEM).

3. Results and discussion

The SEM images in Fig. 1 visualize the surface structure of the three samples. Sample P325 (Fig. 1a) shows the best surface morphology with only a small density of little dips and few deeper holes (e.g. on the lower right side of Fig. 1a). The density

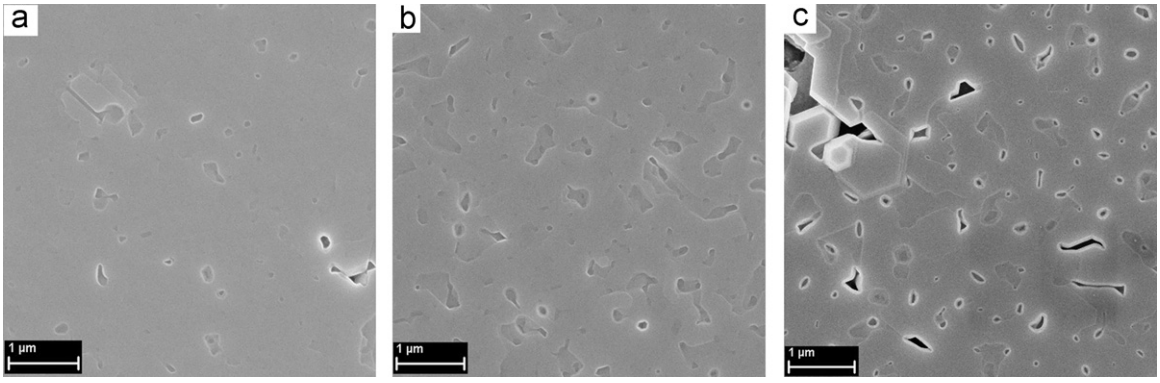

Fig. 1. SEM micrographs of (a) P325, (b) P350 and (c) P375.